Recent Developments on Surface Ground Strain Calculations Due to Underground Mining in Appalachia

Zach G Agioutantis, Professor
Michael Karmis, Professor
Virginia Center For Coal and Energy Research
Virginia Tech
Blacksburg, VA

ABSTRACT

The prediction of ground movements due to underground mining using the influence function method is a mature technology, widely used by researchers and planning engineers around the world. Surface strain, either tensile or compressive, is an important indicator of potential impacts on structures such as buildings, bodies of water, pipelines, railway and power lines, and tailings dams. Calculation of static or dynamic surface strains, for varying surface terrains and slopes, should be accurately predicted and be independent of the methodology applied for the calculation.

This paper discusses and compares the development of horizontal and ground strains on the surface due to underground mining for different surface topologies (sloping terrain, monitoring lines, etc.) and presents the steps needed to ensure accurate calculations. Examples are given to demonstrate how ground strains can be calculated for one- and two-dimensional gridded surfaces.

INTRODUCTION

When the ground surface is digitally represented as a Digital Terrain Model (DTM), it is either in raster form (a grid of squares with a mean value of elevation at the center of the grid cell) or as a vector-based Triangular Irregular Network (TIN). A surface grid can also be constructed starting from a digital TIN model or a digital elevation map. In all such cases, surface elevations are assigned to discrete coordinate pairs (points).

Different analytical models have been proposed to calculate vertical and horizontal displacements on the surface due to underground mining, e.g. SDPS (Agioutantis and Karmis 2013a), CISPM, (Peng, 2008) as well as a number of empirical models, e.g. by Holla and Barclay (2000). Most of the analytical models employ the influence function method for such calculations, which can be easily calibrated to calculate displacements for any mining geometry. Other indices, such as strain, may then be calculated by differentiating this function at specific surface points.

However, calculations do not usually take into account the influence of the surface terrain since the shape of the surface terrain is not available as a continuous mathematical function. To account for the influence of the surface terrain, a continuous function representing surface topography should be available for projecting horizontal displacements prior to calculating strain. In general, small surface areas may be represented using continuous mathematical functions (Agioutantis and Karmis, 2013a), but this is of limited use since these representations only apply locally. As a result, different techniques should be employed for accurate ground strain estimations based on calculated values of surface subsidence and horizontal displacement due to underground mining.

Accurate calculation of surface (ground) strains is important, especially since it is one of the predominant deformation indices used for potential surface structure damage evaluation (Karmis, Agioutantis, and Jarosz, 1995). This paper discusses and compares the development of horizontal and ground strains on the surface due to underground mining for different surface topologies (sloping terrain, monitoring lines, etc.) and presents a methodology for calculating ground strains over one- and two-dimensional surface grids.

CALCULATION OF GROUND DEFORMATIONS USING INFLUENCE FUNCTIONS

Based on the influence function method, in the two- dimensional case, subsidence S(x,s), at any point P(s) due to an infinitesimal excavation, can be expressed by the following equation Karmis et al., 1990):

$$S(x,s) = \frac{1}{r}\int_{-\infty}^{+\infty} So(x)\, e^{\left(-\pi\frac{(x-s)^2}{r^2}\right)} dx \tag{1}$$

and for finite extraction limits (x_1,x_2)

$$S(x,s) = \frac{Smax}{r}\int_{x1}^{x2} e^{\left(-\pi\frac{(x-s)^2}{r^2}\right)} dx \tag{2}$$

where

s = the coordinate of the surface point

x = the coordinate of the infinitesimal excavated element

So(x) = the convergence of the roof of the infinitesimal excavated element

S(x,s) = the subsidence at the surface

x1,x2 = the extents of the excavation

Smax = the maximum expected subsidence over the finite extraction (x_1,x_2)

r = the radius of principal influence =*h*/ tan(β)

h = the overburden depth

β = the angle of principal influence

Furthermore, for the case of a finite size rectangular parcel defined by the coordinates (x_1,y_1-x_2,y_2), equation (3) relates the horizontal displacement *U(x)* to the first derivative of subsidence, and equation (4) relates the horizontal strain *E(x)* to the horizontal displacement (see also Karmis et al., 1990):

$$U(x) = -Bs\frac{\partial S(x,y)}{\partial x} = Bs\frac{Smax}{r^2}\left[e^{\left(-\pi\frac{x_2^2}{r^2}\right)} - e^{\left(-\pi\frac{x_1^2}{r^2}\right)}\right] \times \int_{y_1}^{y_2} e^{\left(-\pi\frac{y^2}{r^2}\right)}dy \quad (3)$$

$$E(x) = \frac{\partial U(x)}{\partial x} = -Bs\,\frac{\partial\left[\frac{\partial S(x,y)}{\partial x}\right]}{\partial x} \quad (4)$$

Where *Bs* is the strain coefficient in length units.

GROUND STRAIN CALCULATIONS ON A FLAT SURFACE FOR POINTS ON A PROFILE

Using this formulation, the strain at any point on the surface can be calculated as a function of mine geometry and overburden parameters. In fact, strain is calculated as the derivative at a single point of a continuous function, which represents the horizontal displacement at a point (see equations (3) and (4)). In such cases, ground strain is usually taken to be equal to the horizontal strain. In addition, it is common to calculate the axial or directional strain for points on a profile line.

The following is presented as a simple example of strain calculations (Figure 1). A transverse line is defined on a flat (horizontal) surface over a panel at an elevation of z=500ft. Extraction thickness is assumed as m=5ft, the supercritical subsidence factor is taken as a=40%, and the edge effect is assumed as d=0ft. Point spacing on the horizontal plane is 20ft. Using default parameters for the influence angle (β) and for the strain coefficient (*Bs*) as determined for the eastern Appalachian Coalfields (Agioutantis and Karmis, 2013a), subsidence, horizontal displacement, and strain are calculated and shown in Figure 2. In this case, horizontal strain and directional strain along this transverse half profile are equal and are depicted as EX in Figure 2.

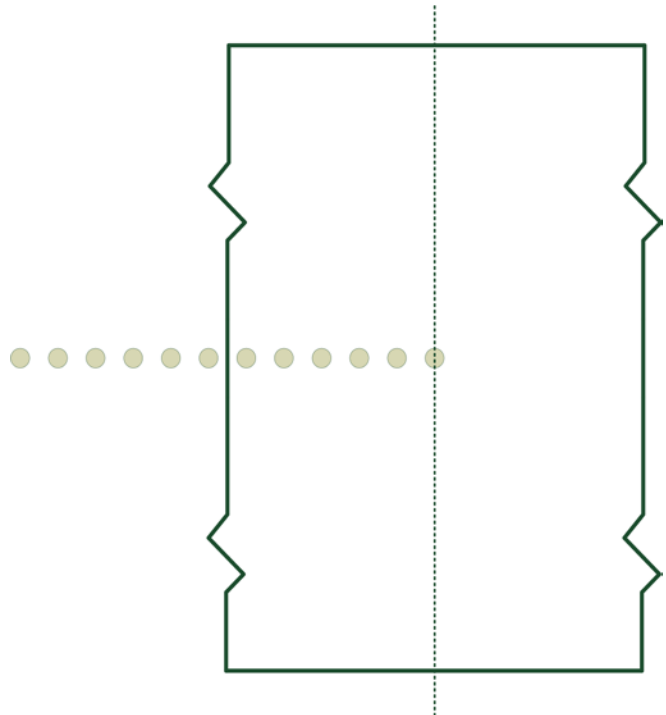

Figure 1. Plan view of example case study - rectangular extraction and transverse monitoring line.

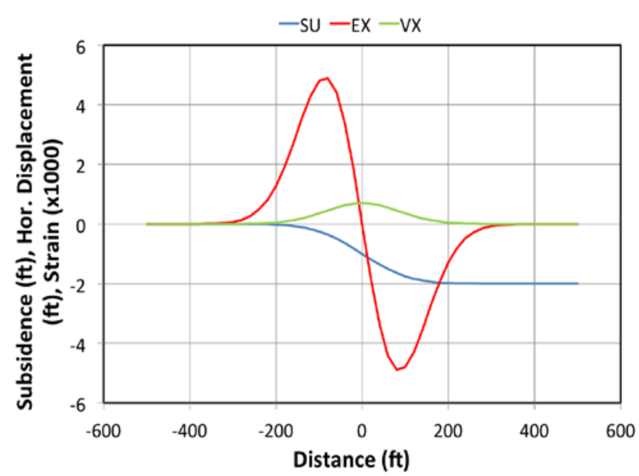

Figure 2. Calculated subsidence (SU), Horizontal Strain (EX), and Horizontal Displacement (VX) along the transverse monitoring line.

The axial strain is calculated using strain rotation for each monitoring point, as shown schematically in Figure 3. Axial strain values are calculated for each individual point. The directional vector is calculated by connecting each pair of consecutive points with a straight line. For the last point in the sequence, the directional vector calculated for the previous point may be applied.

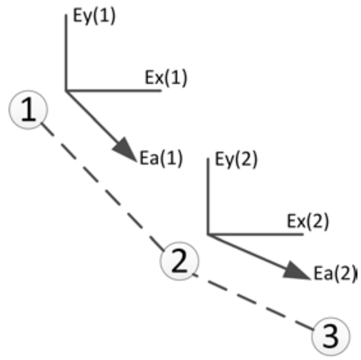

Figure 3. Axial strain along monitoring line points (points are shown in plan view).

GROUND STRAIN CALCULATIONS ON AN IRREGULAR SURFACE FOR POINTS ON A PROFILE

Ground deformation monitoring line points rarely lie on a horizontal surface. Thus, when the monitoring profile covers an irregular surface, the projection of the horizontal displacement (and the horizontal strain) on the ground surface varies and depends on the shape of the surface. Assuming that only the pre-mining elevations of the profile points are known, ground strain can be calculated at every point (Pi) of the profile as follows (Figure4):

Temporary points A and B should be defined at mid-distance between points P(i-1), P(i) and P(i) and P(i+1) using pre-mining coordinate information (x(i), y(i), z(i), etc.) for points P(i-1), P(i), and P(i+1), as shown in Figure 4. The distance between *A* and *B* is calculated as w = ||A - B||

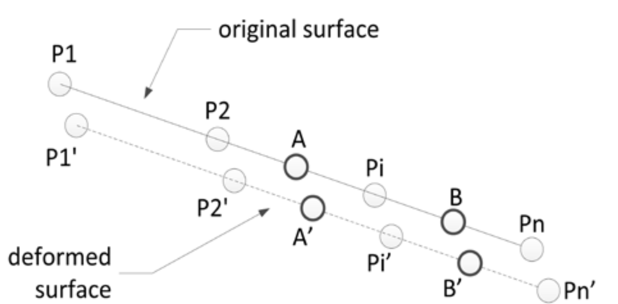

Figure 4. Surface monitoring points on a sloping terrain (points are shown in cross section view).

$$A = \left[\frac{x(i)+x(i-1)}{2}, \frac{y(i)+y(i-1)}{2}, \frac{z(i)+z(i-1)}{2}\right] \tag{5}$$

$$B = \left[\frac{x(i)+x(i+1)}{2}, \frac{y(i)+y(i+1)}{2}, \frac{z(i)+z(i+1)}{2}\right] \tag{6}$$

The procedure is repeated for points *A'* and *B'* at the deformed surface using the coordinates at the deformed state (i.e., *x(i)* + *δx(i), y(i)* + *δy(i), z(i)* + *δz(i)*). The distance between *A'* and *B'* is then calculated as *w'* = ||*A'* - *B'*|| Ground strain *EG* at point (*i*) is then calculated as follows:

$$EG(i) = \frac{w' - w}{w} = \frac{w'}{w} - 1 \tag{7}$$

Another approach commonly employed by surveyors monitoring surface points is to calculate strains for the midpoints of the linear segments between points. That means that although horizontal and vertical displacements are available for points P(i-1), P(i), P(i+1), horizontal and ground strains are calculated for points *A* and *B*. With the approach highlighted above, strains are available for the actual monitoring points.

Figure 5 compares ground strain and horizontal strain calculated for the example shown in Figure 1, where the surface is sloping to the east by five degrees (or 5.6%). It is easily determined that the tensile strains increase on the uphill side while they tend to decrease when moving downhill. This is a well-known behavior and has already been documented by case studies. For example, Khair, Quinn, and Chaffins (1987) postulate that measured strains indicate that there is a significant increase in ground tensile strain when mining in a direction that approaches uphill topography. These amounts decrease when approaching the downhill slope side.

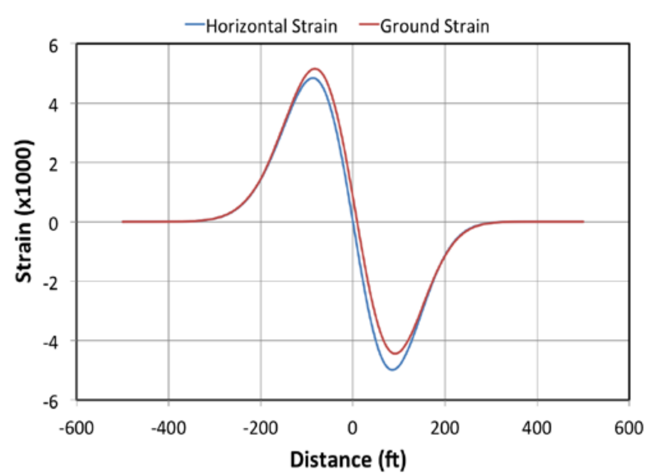

Figure 5. Comparison of ground and horizontal strain for a 5 degree sloping surface (surface point spacing = 20 ft).

Figure 6 compares the calculated ground strain for the same example where each line corresponds to different point spacing for the surface points, P(i). It can be easily determined that for coarse point spacing, an error for the maximum calculated ground strain value up to 20 or 25% may be introduced.

In fact, the above adjustments can be applied to strain calculations of relatively uniform surfaces, which are deformed by underground mining operations. In the following example, the monitoring line over a longwall panel in southwest Pennsylvania was modeled, as shown in Figure 7. Calculations were performed using the Surface Deformation Prediction System software package

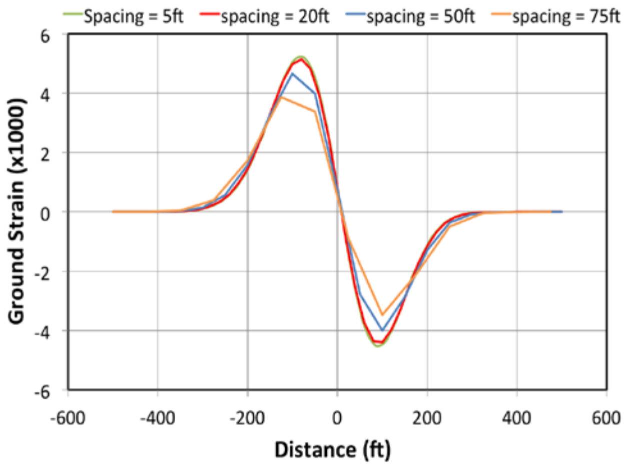

Figure 6. Comparison of ground strain curves on a 5 degree sloping surface for different surface point spacing values ranging from 5 to 75 ft.

(SDPS) (Agioutantis and Karmis, 2013a), assuming default parameters for the Appalachian coalfields and a hardrock amount of 27%. Figure 8 compares measured values, values for axial horizontal strain and values for ground strain, calculated, shown in equation 7. As can be easily observed, the axial strain calculation over predicts the measured strain profile.

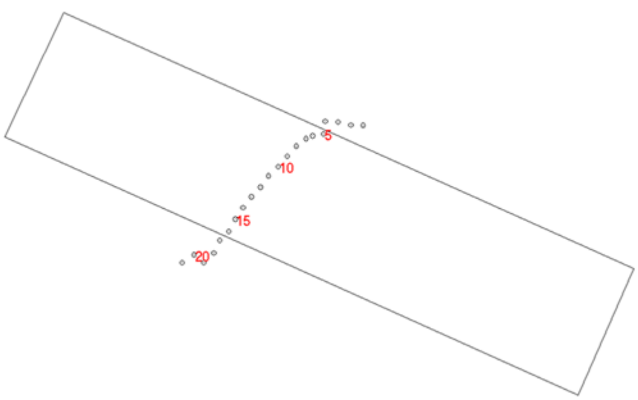

Figure 7. Layout of monitoring line over a longwall panel in Pennsylvania.

GROUND STRAIN CALCULATIONS WHEN SURFACE TOPOGRAPHY INFORMATION IS AVAILABLE

The surface topography over undermined areas is usually available as contour lines of different density. Using commercially available software, such as Carlson Software or Surfer, it is easy to convert these contour lines to grid files with appropriate density. For example, if topography is represented by 20-ft contour lines, the grid cell size of the surface grid should be on the order of 20 ft. Although gridding software may calculate grids of squares or rectangles, it is recommended to develop grids with square cells.

After developing the surface topography grid, ground deformations may be calculated for each grid point. Figure 9a shows a four square cell arrangement comprising nodes

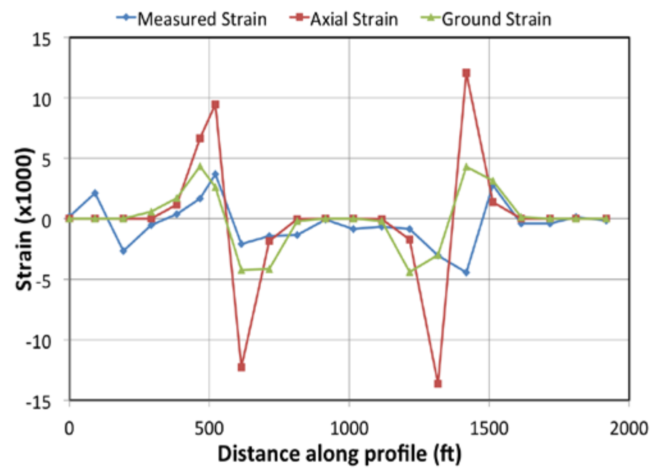

Figure 8. Comparison of measured, axial and ground strains along monitoring line profile.

A,B,C,D,E,F,G,H,X. In typical surface deformation calculations and when the surface points are within the influence area of the extracted panel, each of these nodes will undergo vertical and horizontal movements (Figure 9b). Using equation (4), the horizontal strain at each point may be easily calculated. However, ground strain cannot be calculated analytically, unless the deformed surface comprising these four square cells is defined. Alternatively, the maximum ground strain experienced at the center point (X) may be calculated using the following methodology.

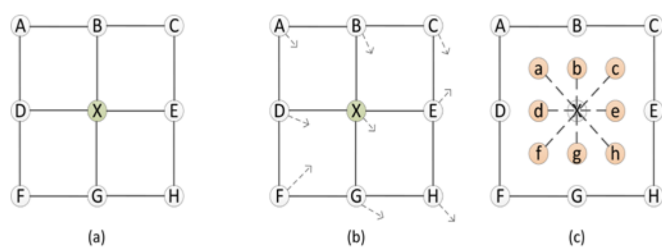

Figure 9. Calculating ground strain for point (X) using temporary points.

Temporary surface points a,b,c,d,e,f,g,h should be considered, which lie at the midpoint of the vertical, horizontal and diagonal connectors between the nodes around point X (Figure 9c). The ground strain due to compression or tension can be calculated along lines a-h, b-g, c-f, d-e using equations similar to (5) and (6) and selecting the maximum value as the maximum ground strain. Using the same procedure, ground strain at different directions may be calculated. Thus, the maximum ground strain can be calculated for point X based on the calculation of horizontal and vertical movements at this and neighboring points and information regarding the topography of the terrain.

INFLUENCE OF SLOPING TERRAIN ON GROUND STRAIN CALCULATIONS

Figure 10 shows a second example of a mined panel under sloping terrain. A perfect hill has been simulated over the right rib of the panel and about the middle lengthwise. The base elevation of the hill is 400 ft, and the apex is 600 ft above the mined seam.

The surface over all of the remaining undermined area is set to an elevation of 400 ft. All other parameters are the same as in the previous example. Maximum horizontal strain and maximum ground strain were calculated over the entire area (Figures11 and 12). Contour line magnitudes are lower around the hill area in the case of the ground strain plots (Figure12).

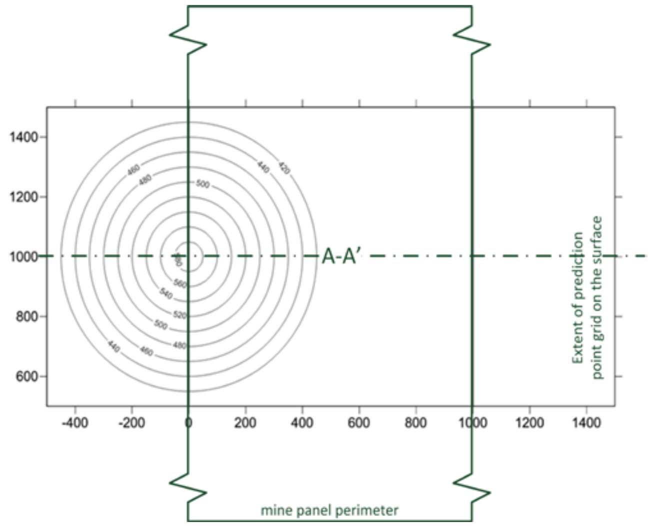

Figure 10. Synthetic mine plan and surface topography representing sloping terrain.

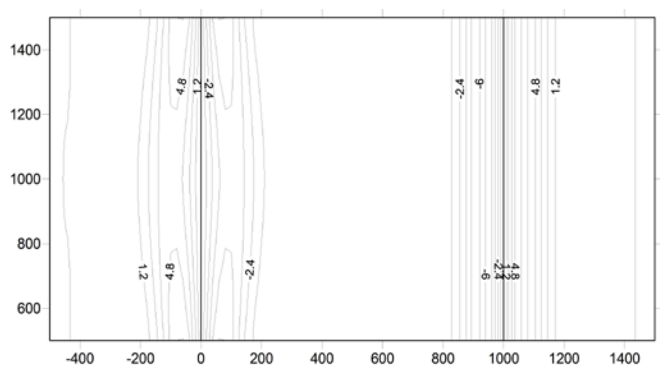

Figure 11. Maximum horizontal strain contours.

In addition, a cross-section comparing horizontal strain and ground strain along line A-A' is plotted in Figure 13. There is definitely a reduction in ground strain magnitudes over the hilly area. In particular, strains may even reverse (i.e., tensile to compressive to tensile and vice versa) under sudden changes of topography.

CONCLUSIONS

This paper discusses strain calculations for different topologies of surface points (flat surfaces, flat monitoring lines, monitoring lines on irregular terrain, sloping grids, etc.). A comparison between axial horizontal strain and axial ground strain for an actual case study shows that ground strain predictions will more accurately reflect the measured profile, while axial horizontal strain calculations can over predict the strain regime. The comparison between horizontal strain and ground strain shows that ground strain is greatly affected by the topography of the terrain and that, in some cases, local reversals of strain conditions may occur.

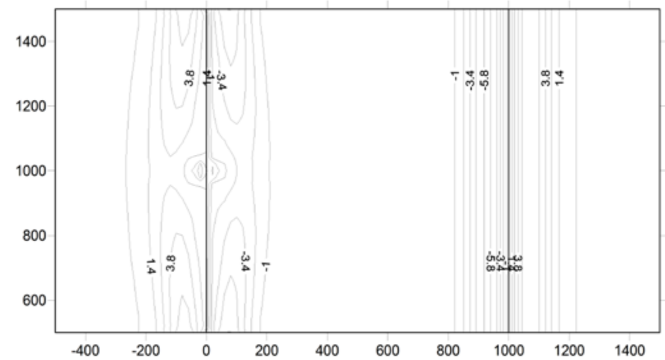

Figure 12. Maximum ground strain contours.

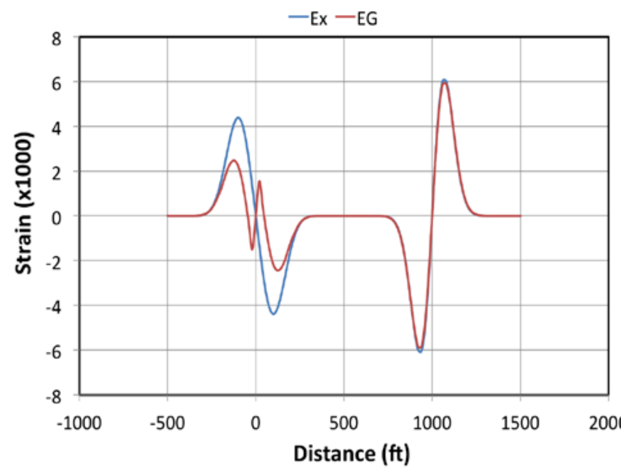

Figure 13. Comparison of horizontal strain (Ex) and ground strain (EG) along line A-A';.

All calculation tools and procedures have been implemented into the Influence function formulation program of the SDPS software package (Agioutantis and Karmis, 2013a). Work is underway to validate the procedure introduced for ground strain adjustment based on a grid of points representing the terrain around the monitoring line. Also, further research is needed to calculate ground strain under dynamic conditions (i.e., as a function of panel advance).

ACKNOWLEDGEMENTS

This study was sponsored by the Appalachian Research Initiative for Environmental Science (ARIES). ARIES is an industrial affiliates program at Virginia Tech, supported by members that include companies in the energy sector. The research under ARIES is conducted by independent researchers in accordance with the policies on scientific integrity of their institutions. The views, opinions and recommendations expressed herein are solely those of the authors and do not imply any endorsement by ARIES employees, other ARIES-affiliated researchers or industrial members. Information about ARIES can be found at http://www.energy.vt.edu/ARIES.

REFERENCES

Agioutantis, Z. and Karmis, M. (2013a). *Surface Deformation Prediction System for Windows version 6.1i, Quick Reference Guide and Working Examples*. Blacksburg, Virginia: Virginia Polytechnic Institute and State University, pp. 273.

Agioutantis, Z. and Karmis, M. (2013b). "Addressing the effect of sloping terrain on ground movements due to underground mining." In: Environmental Considerations in Energy Production. Edited by J. Craynon, Society for Mining, Metallurgy, & Exploration. Englewood, Colorado, 308-318.

Holla, L. and Barclay E. (2000). *Mine Subsidence in the Southern Coalfield, NSW, Australia*. Sydney, New South Wales Department of Mineral Resources, 118 p.

Karmis, M., Agioutantis, Z. and Jarosz, A. (1990). "Recent developments in the Application of the influence function method for ground movement predictions in the U.S. " *Mining Science and Geotechnology. 10*: 233–245.

Karmis, M., Mastoris, J. and Agioutantis, Z. (1995). "Potential of the "damage angle" concept for assessing surface impacts of underground mining. " *SME Transactions. 296*: 1883–1886.

Khair, A.W., Quinn, M.K. and Chaffins, R.D. (1987). «Effects of topography on ground movement due to longwall mining. « In: *Proceedings of the SME-AIME Annual Meeting*.Englewood, CO: Society for Mining, Metallurgy, & Exploration. Preprint No. 87-142, pp. 10.

Peng, S.S. (2008). "*Coal Mine Ground Control, Third Edition,*" Published by S.S. Peng, 764p.